Supplement of Biogeosciences, 22, 5833–5848, 2025 https://doi.org/10.5194/bg-22-5833-2025-supplement © Author(s) 2025. CC BY 4.0 License.





Supplement of

The use of newly assimilated photosynthates by soil autotrophic and heterotrophic respiration on a diurnal scale

Moeka Ono et al.

Correspondence to: Moeka Ono (mono@tamu.edu) and Asko Noormets (noormets@tamu.edu)

The copyright of individual parts of the supplement might differ from the article licence.

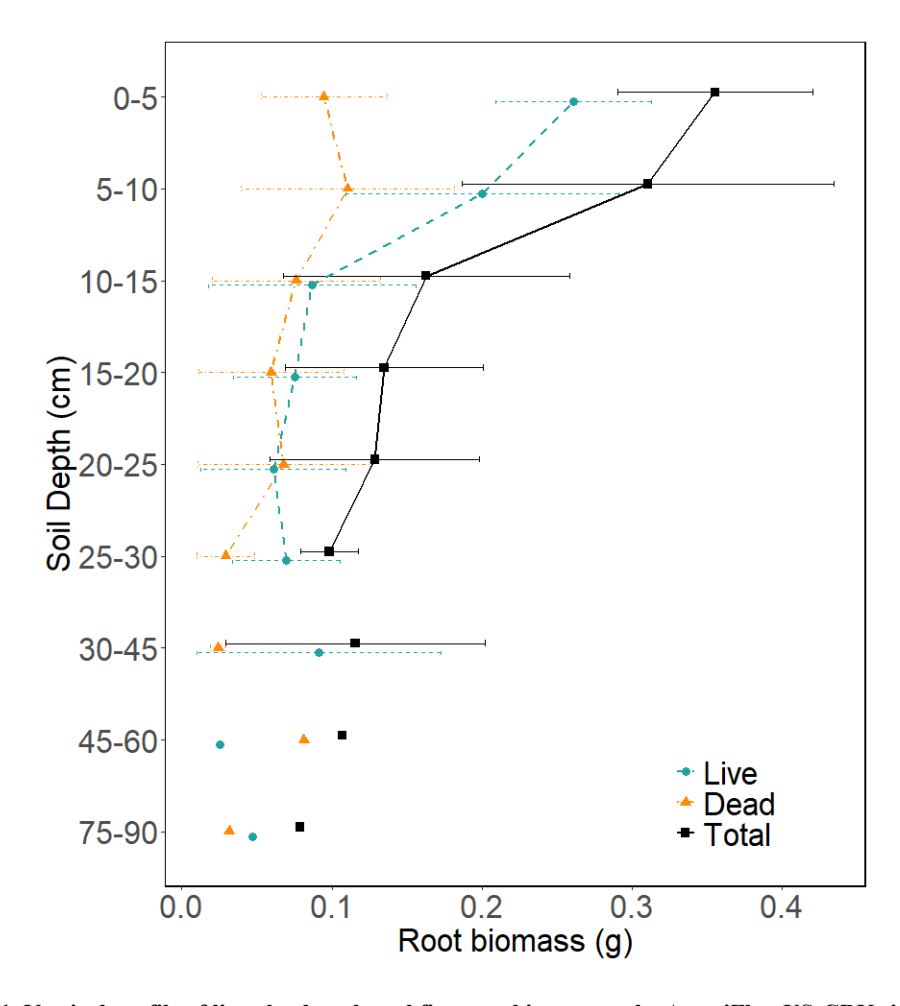


Figure. S1. Vertical profile of live, dead, and total fine root biomass at the AmeriFlux US-CRK site in February 2023. Error bars represent standard deviation among plots (n = 4).

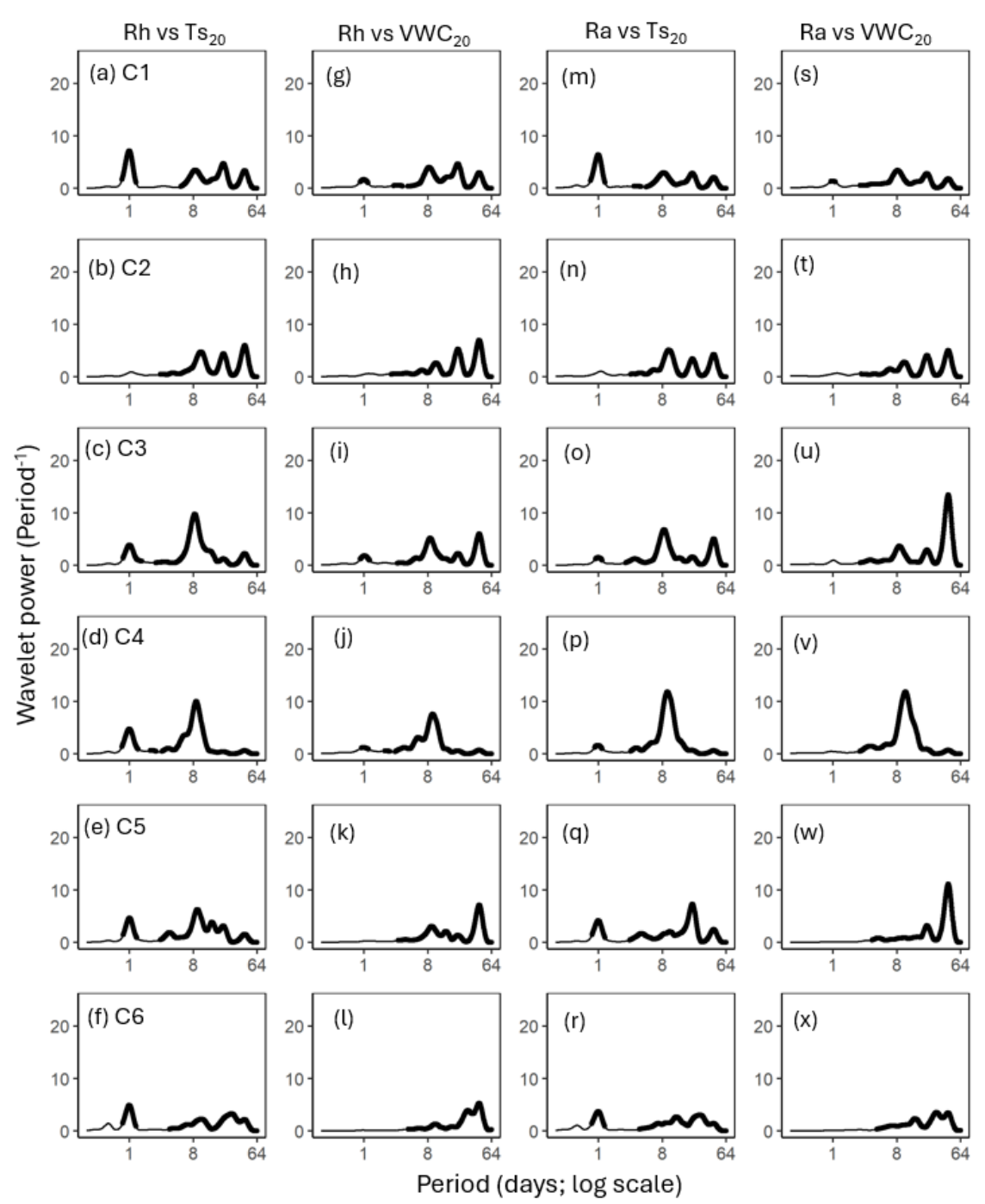


Figure S2. Average wavelet power in the frequency domain (Period; time intervals from 6 h to 64 d) generated from the cross-wavelet transformation of heterotrophic respiration (Rh) against soil temperature (T_{820} ; a-f) and volumetric water content (VWC₂₀; g-l) at 20 cm depth, and autotrophic respiration (Ra) against T_{820} (m-r) and VWC₂₀ (s-x) for six campaigns (C1-C6) at the US-CRK site. The bold contours indicate areas with significant coherence at the 5% level against white noise.

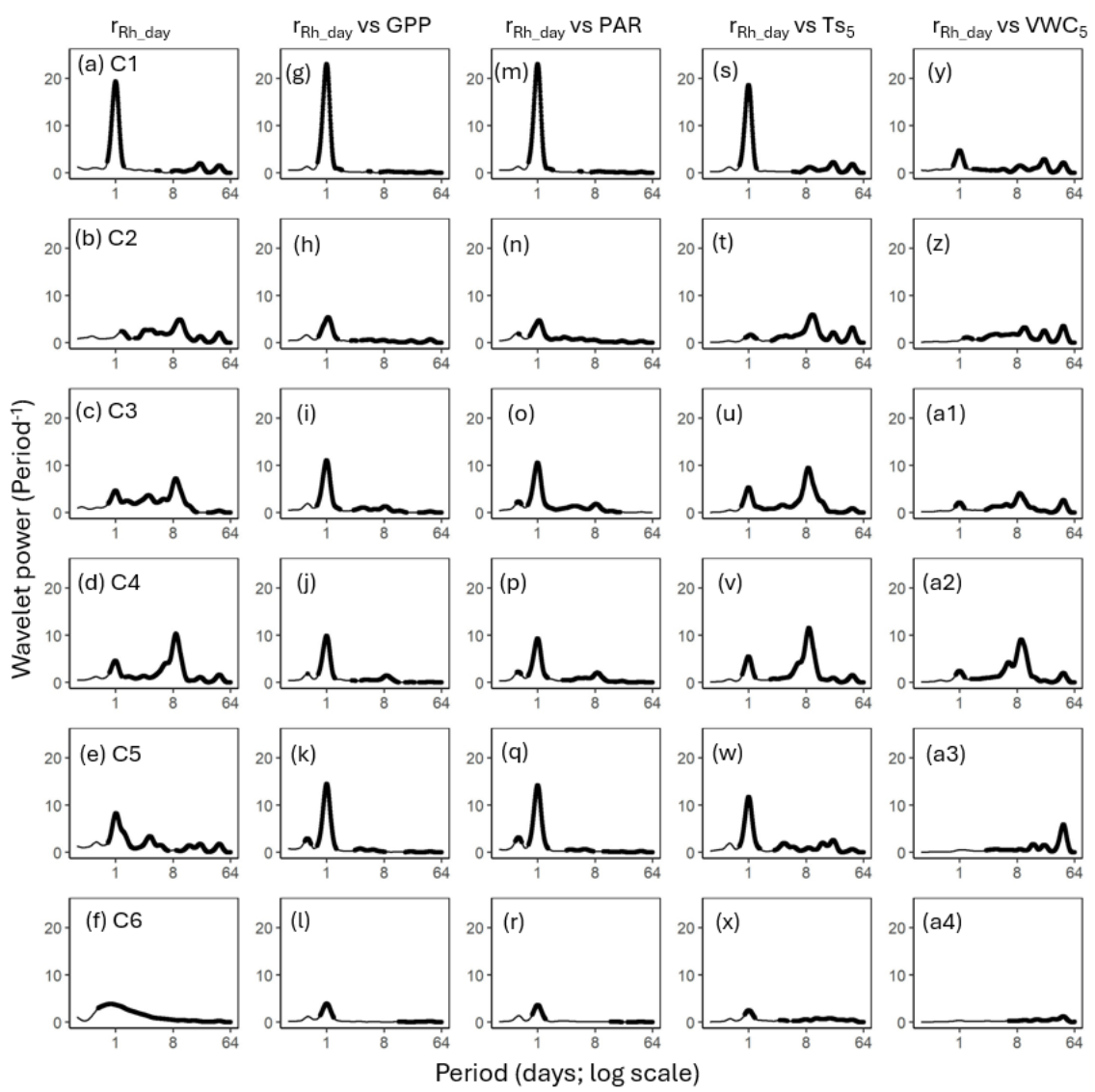


Figure S3. Average wavelet power in the frequency domain (Period; time intervals from 6 h to 64 d) generated from the wavelet transformation of the model residual of heterotrophic respiration with coefficients estimated by a daily window (r_{Rh_day} ; a-f) for six campaigns (C1–C6) at US-CRK. Average wavelet power in the frequency domain generated from the cross-wavelet transformation of r_{Rh_day} against gross primary productivity (GPP; g-1), photosynthetically active radiation (PAR; m-r), soil temperature (T_{S5} ; s-x), and volumetric water content (VWC5; y-a4) at 5 cm depth for six campaigns at the US-CRK site. The bold contours indicate areas with significant coherence at the 5% level against white noise.

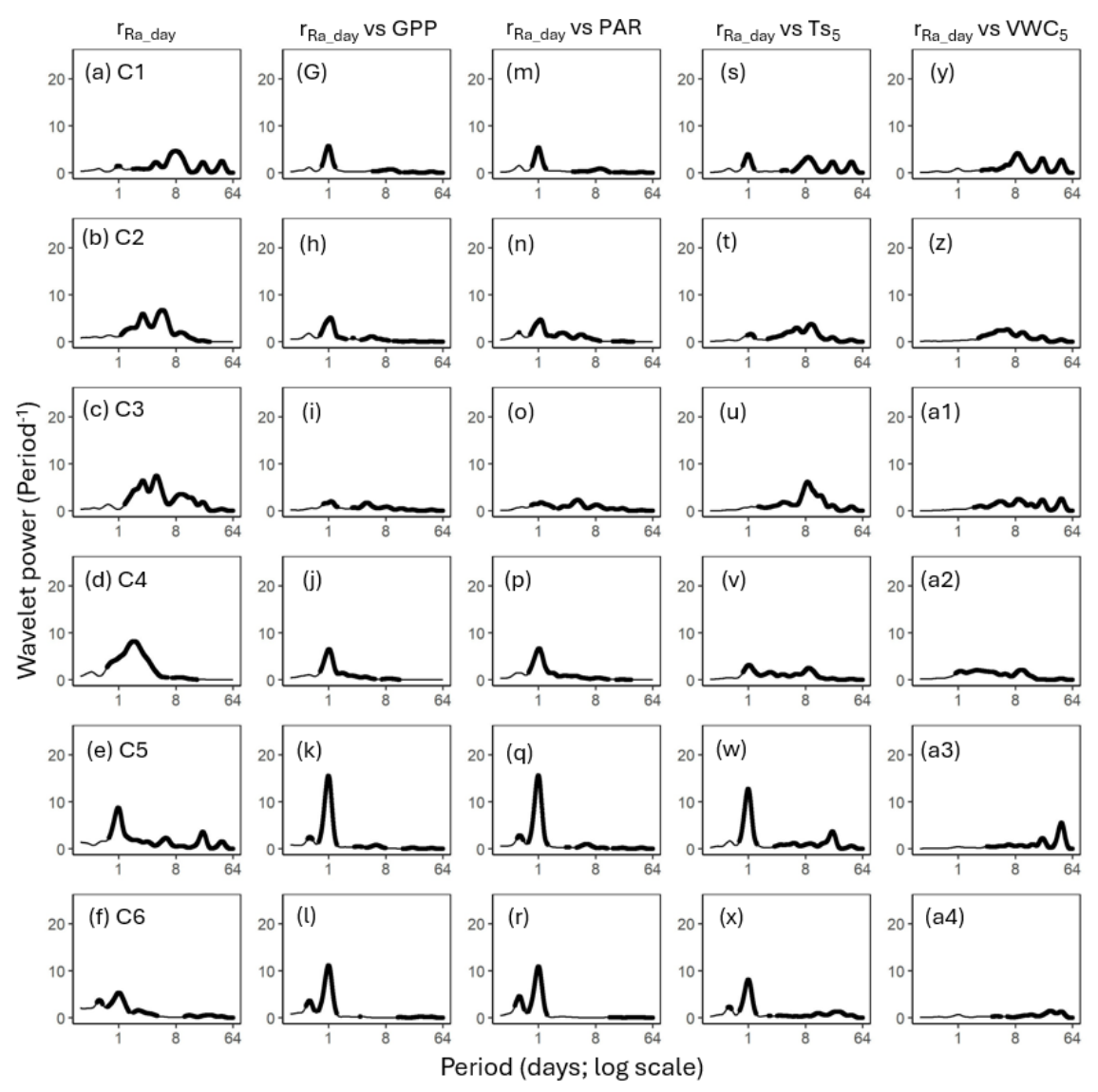


Figure S4. Average wavelet power in the frequency domain (Period; time intervals from 6 h to 64 d) generated from the wavelet transformation of the model residual of autotrophic respiration with coefficients estimated by a daily window (r_{Ra_day} ; a–f) for six campaigns (C1–C6) at US-CRK. Average wavelet power in the frequency domain generated from the cross-wavelet transformation of r_{Ra_day} against gross primary productivity (GPP; g–l), photosynthetically active radiation (PAR; m–r), soil temperature (T_{S5} ; s–x), and volumetric water content (VWC5; y–a4) at 5 cm depth for six campaigns at the US-CRK site. The bold contours indicate areas with significant coherence at the 5% level against white noise.

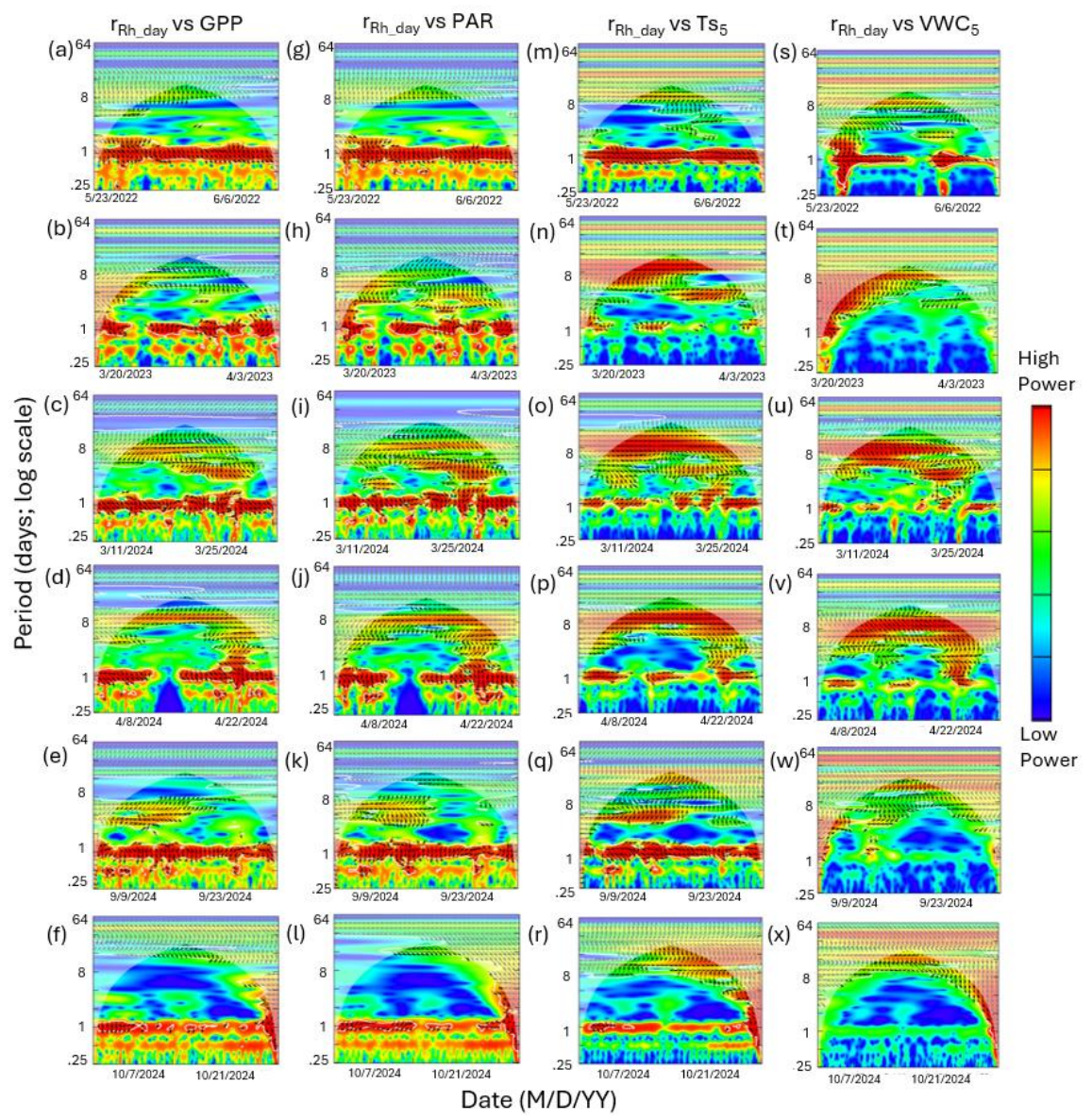


Figure S5: Heatmaps of the cross-wavelet transformation (XWT) of model residual of heterotrophic respiration with coefficients estimated by a daily window (r_{Rh_day}) against gross primary productivity (GPP; a-f), photosynthetically active radiation (PAR; g-l), soil temperature (T_{SS} ; m-r), and volumetric water content (VWC₅; s-x) at 5 cm depth for six measurement campaigns (C1-C6) at US-CRK. Arrows pointing to the right and left represent positive and negative correlations, respectively, without lag. Arrows pointing up-left (positive correlation) and down-right (negative correlation) indicate the response component lags behind the driver, while arrows pointing up-right and down-left indicate that the driver lags behind the response component. The 5% significance level of the XWT analysis was generated within the cone of influence (COI) against white noise and identified by white contour lines. COI within the heat plot is identified with a light shade.

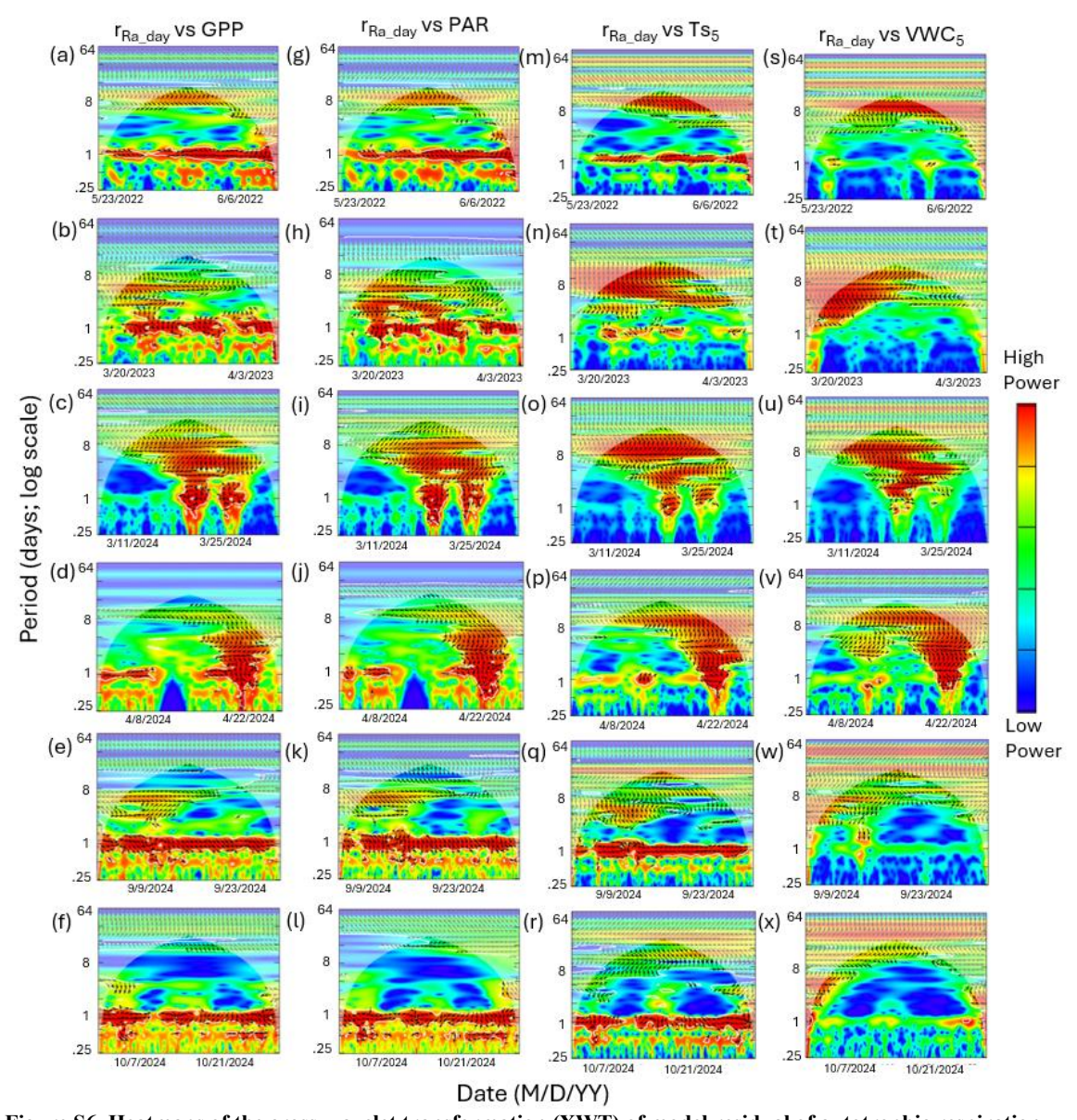


Figure S6. Heatmaps of the cross-wavelet transformation (XWT) of model residual of autotrophic respiration with coefficients estimated by a daily window (r_{Ra_day}) against gross primary productivity (GPP; a-f), photosynthetically active radiation (PAR; g-l), soil temperature (T_{SS} ; m-r), and volumetric water content (VWC₅; s-x) at 5 cm depth for six measurement campaigns (C1-C6) at US-CRK. Arrows pointing to the right and left represent positive and negative correlations, respectively, without lag. Arrows pointing up-left (positive correlation) and down-right (negative correlation) indicate the response component lags behind the driver, while arrows pointing up-right and down-left indicate that the driver lags behind the response component. The 5% significance level of the XWT analysis was generated within the cone of influence (COI) against white noise and identified by white contour lines. COI within the heat plot is identified with a light shade.

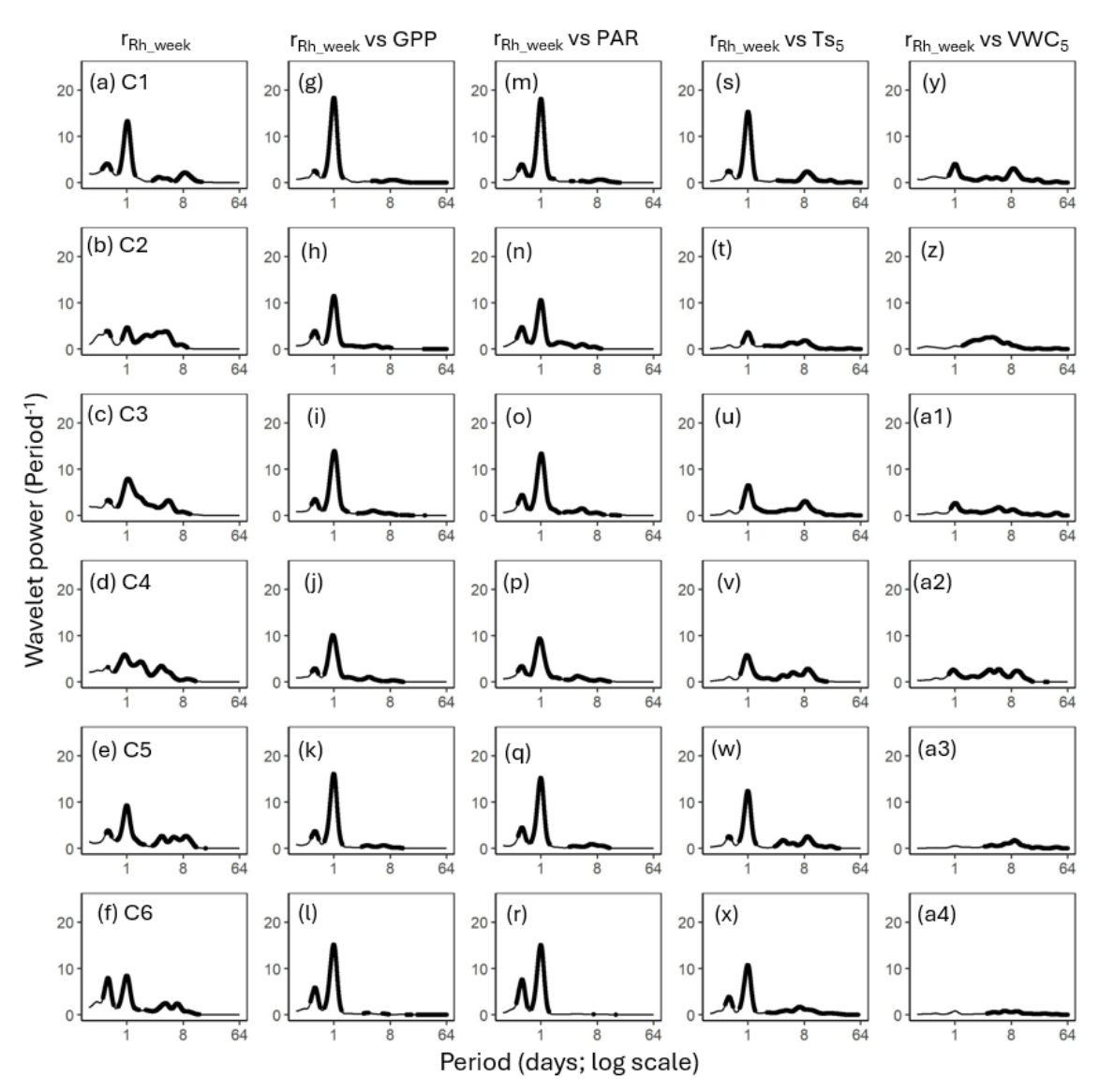


Figure S7. Average wavelet power in the frequency domain (Period; time intervals from 6 h to 64 d) generated from the wavelet transformation of the model residual of heterotrophic respiration with coefficients estimated by a weekly rolling window (r_{Rh_week} ; a-f) for six campaigns (C1-C6) at US-CRK. Average wavelet power in the frequency domain generated from the cross-wavelet transformation of r_{Rh_week} against gross primary productivity (GPP; g-l), photosynthetically active radiation (PAR; m-r), soil temperature (T_{SS} ; s-x), and volumetric water content (VWC₅; y-a4) at 5 cm depth for six campaigns at the US-CRK site. The bold contours indicate areas with significant coherence at the 5% level against white noise.

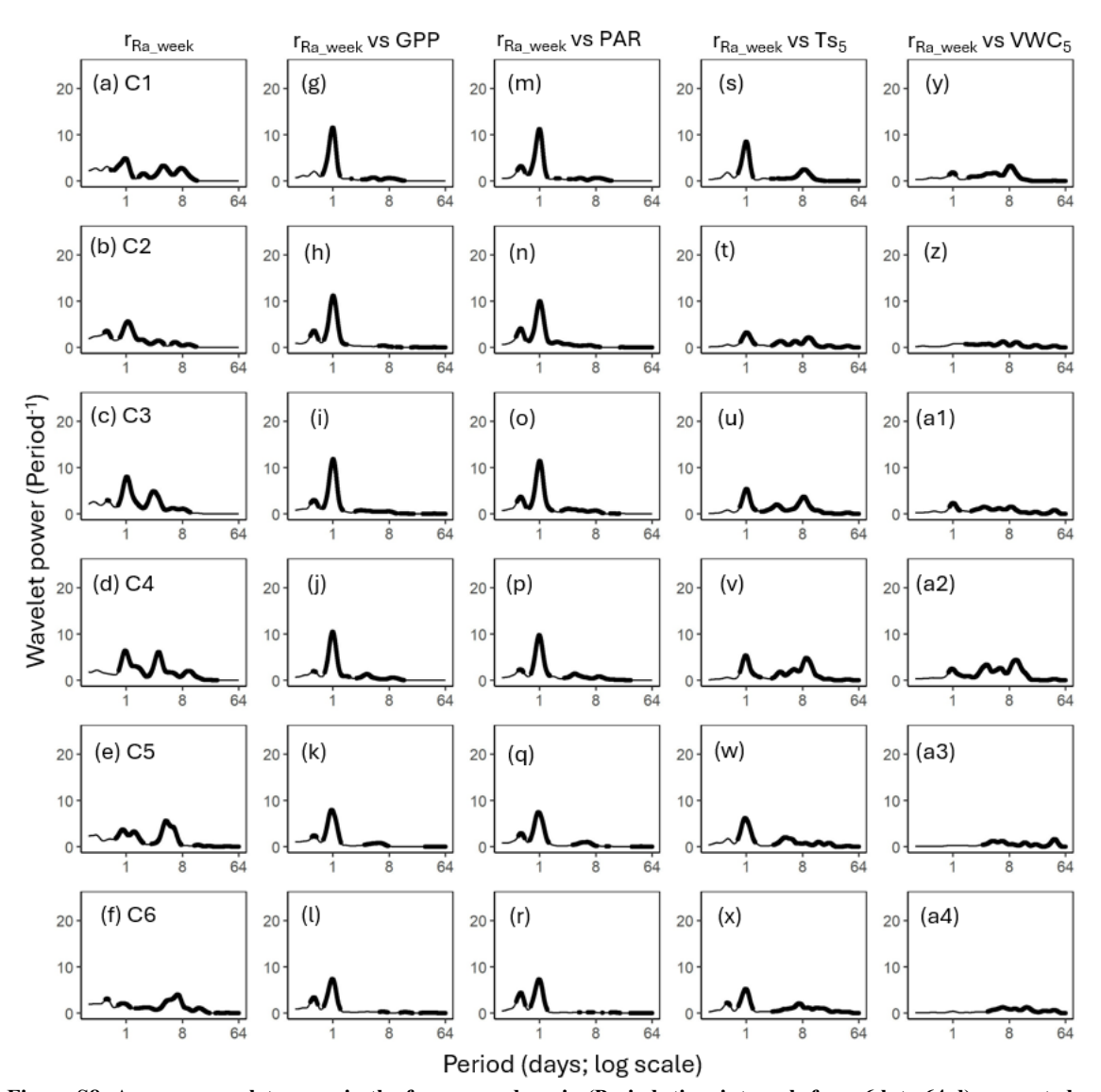


Figure S8. Average wavelet power in the frequency domain (Period; time intervals from 6 h to 64 d) generated from the wavelet transformation of the model residual of autotrophic respiration with coefficients estimated by a weekly rolling window (r_{Ra_week} ; a–f) for six campaigns (C1–C6) at US-CRK. Average wavelet power in the frequency domain generated from the cross-wavelet transformation of r_{Ra_week} against gross primary productivity (GPP; g–l), photosynthetically active radiation (PAR; m–r), soil temperature (T_{SS} ; s–x), and volumetric water content (VWC₅; y–a4) at 5 cm depth for six campaigns at the US-CRK site. The bold contours indicate areas with significant coherence at the 5% level against white noise.

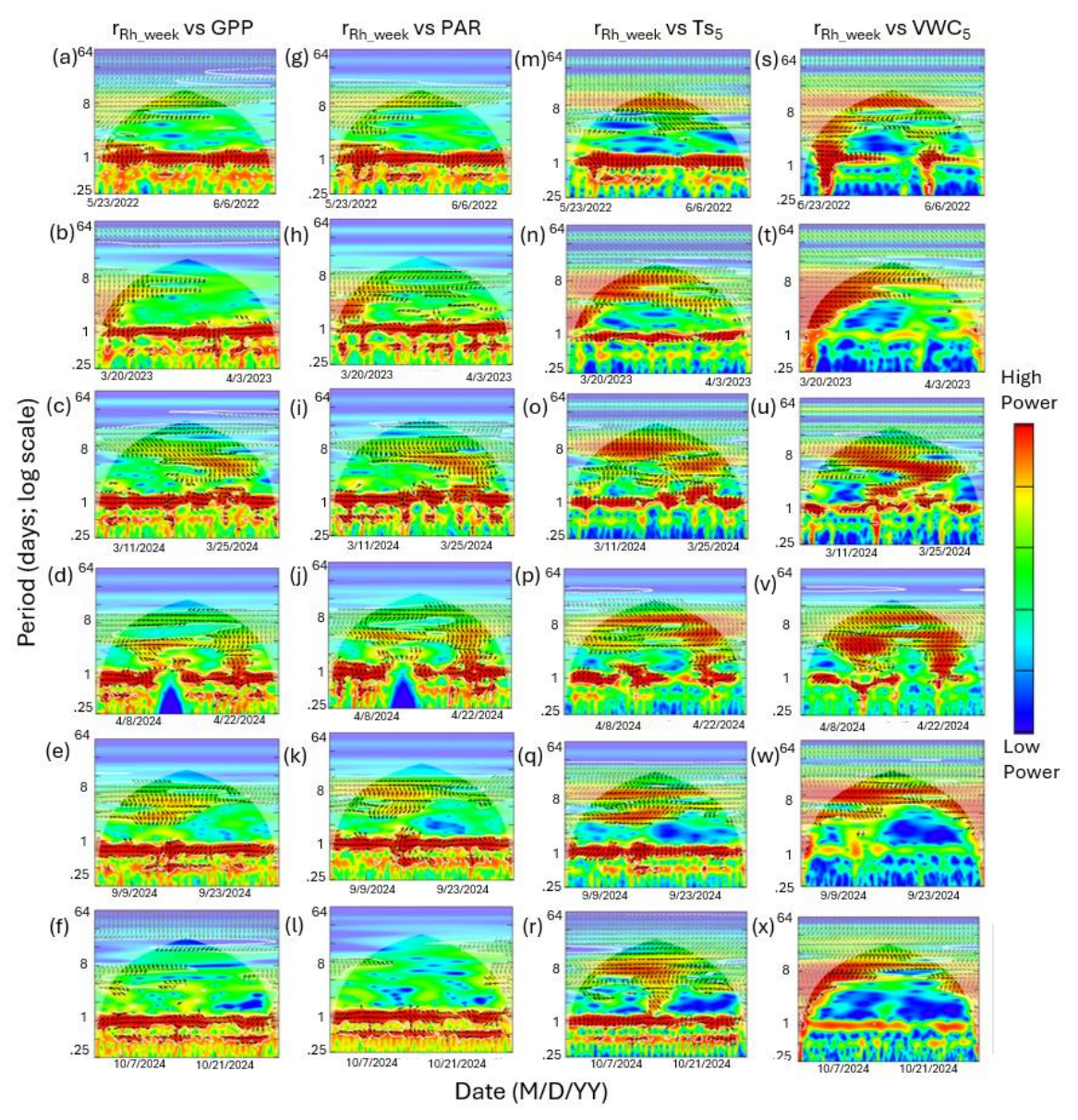


Figure S9. Heatmaps of the cross-wavelet transformation (XWT) of model residual of heterotrophic respiration with coefficients estimated by a weekly rolling window (r_{Rh_week}) against gross primary productivity (GPP; a-f), photosynthetically active radiation (PAR; g-l), soil temperature (T_{SS} ; m-r), and volumetric water content (VWC₅; s-x) at 5 cm depth for six measurement campaigns (C1-C6) at US-CRK. Arrows pointing to the right and left represent positive and negative correlations, respectively, without lag. Arrows pointing up-left (positive correlation) and down-right (negative correlation) indicate the response component lags behind the driver, while arrows pointing up-right and down-left indicate that the driver lags behind the response component. The 5% significance level of the XWT analysis was generated within the cone of influence (COI) against white noise and identified by white contour lines. COI within the heat plot is identified with a light shade.

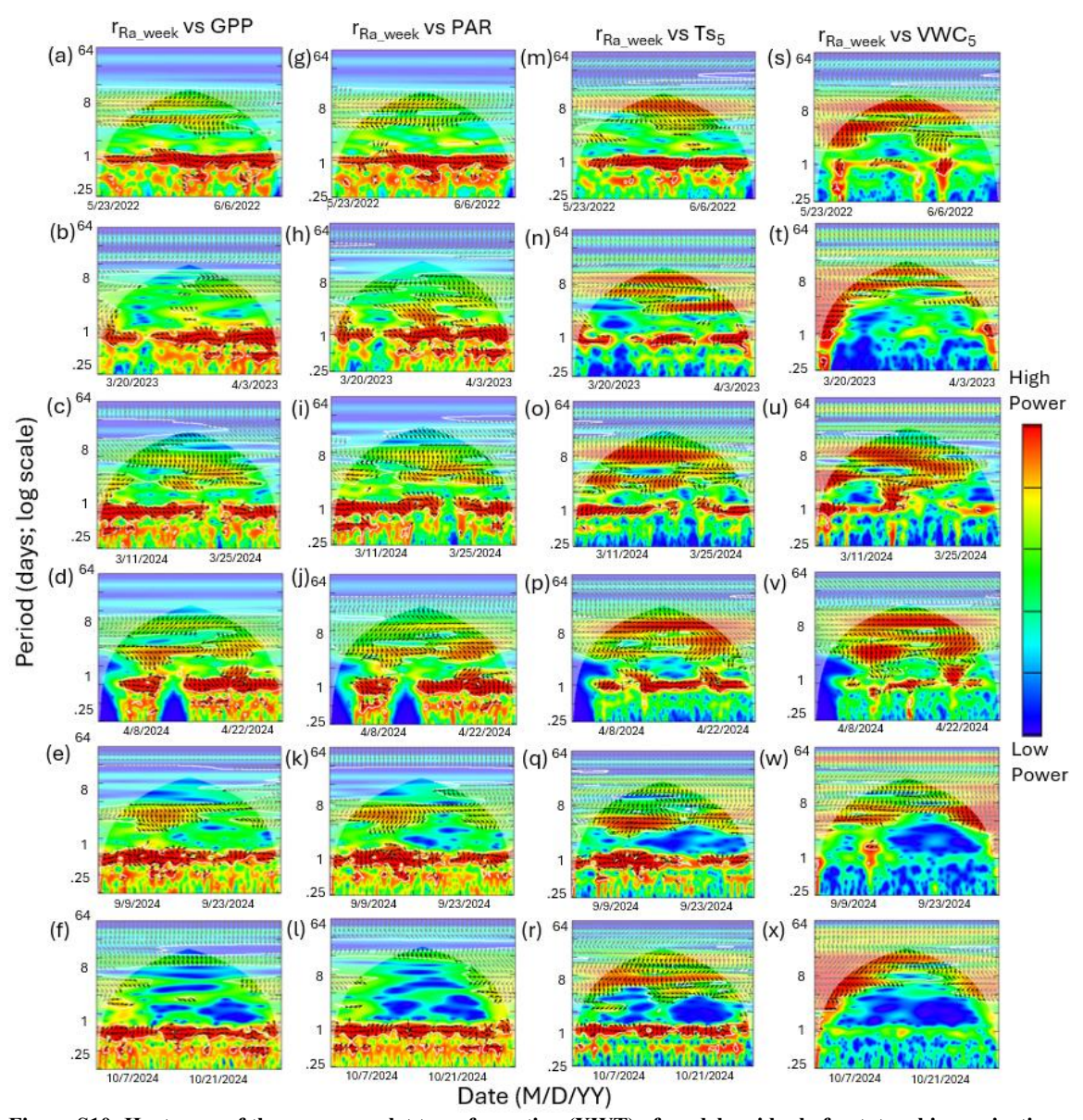


Figure S10. Heatmaps of the cross-wavelet transformation (XWT) of model residual of autotrophic respiration with coefficients estimated by a weekly rolling window (r_{Ra_week}) against gross primary productivity (GPP; a-f), photosynthetically active radiation (PAR; g-l), soil temperature (T_{S5} ; m-r), and volumetric water content (VWC₅; s-x) at 5 cm depth for six measurement campaigns (C1–C6) at US-CRK. Arrows pointing to the right and left represent positive and negative correlations, respectively, without lag. Arrows pointing up-left (positive correlation) and down-right (negative correlation) indicate the response component lags behind the driver, while arrows pointing up-right and down-left indicate that the driver lags behind the response component. The 5% significance level of the XWT analysis was generated within the cone of influence (COI) against white noise and identified by white contour lines. COI within the heat plot is identified with a light shade.

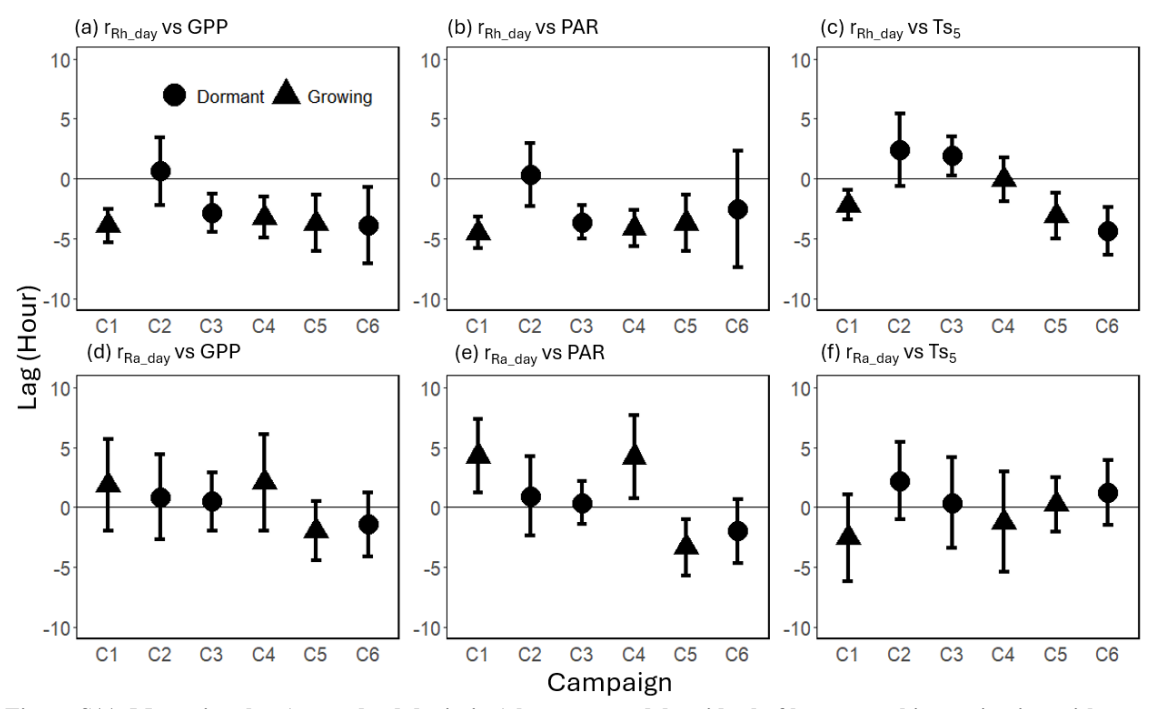


Figure S11. Mean time lag (\pm standard deviation) between model residual of heterotrophic respiration with coefficients by each day (r_{Rh_day}) and (a) gross primary productivity (GPP), (b) photosynthetically active radiation (PAR), and (c) soil temperature (Tss), and between model residual of autotrophic respiration with coefficients estimated by a daily window (r_{Ra_day}) and (d) GPP, (e) PAR, and (f) Tss at the diurnal frequency range (0.5 to 1.5 d) across six measurement campaigns (C1–C6). Phase differences were averaged over the diurnal frequency range and included only when the 1 d spectral peak was significant (p < 0.1). Round dots represent dormant season campaigns, while triangles represent growing season campaigns. Positive lag values indicate that respiration preceded the corresponding driver, while negative values indicate that respiration lagged behind the driver.

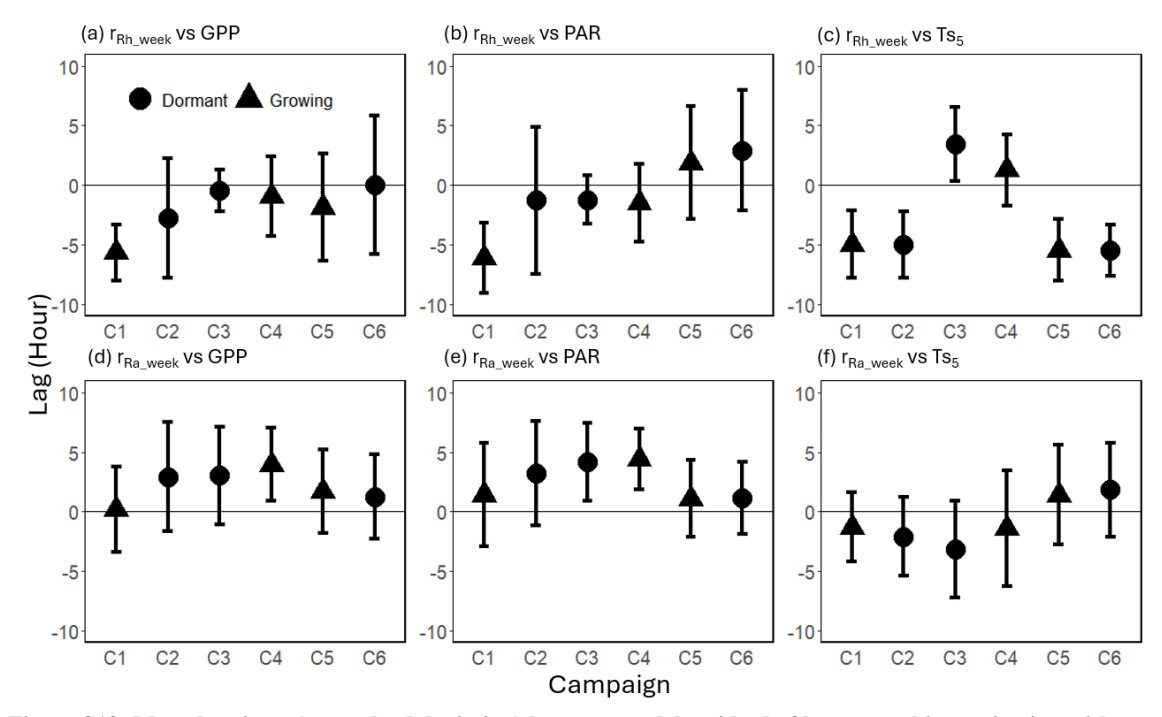


Figure S12. Mean lag times (\pm standard deviation) between model residual of heterotrophic respiration with coefficients estimated by a weekly rolling window (r_{Rh_week}) and (a) gross primary productivity (GPP), (b) photosynthetically active radiation (PAR), and (c) soil temperature (T_{SS}), and between model residual of autotrophic respiration with coefficients estimated by weekly rolling windows (r_{Ra_week}) and (d) GPP, (e) PAR, and (f) T_{SS} at the diurnal frequency range (0.5 to 1.5 d) across six measurement campaigns (C1–C6). Phase differences were averaged over the diurnal frequency range and included only when the 1 d spectral peak was significant (p < 0.1). Circular dots represent dormant season campaigns, while triangles represent growing season campaigns. Positive lag values indicate that respiration preceded the corresponding driver, while negative values indicate that respiration lagged behind the driver.

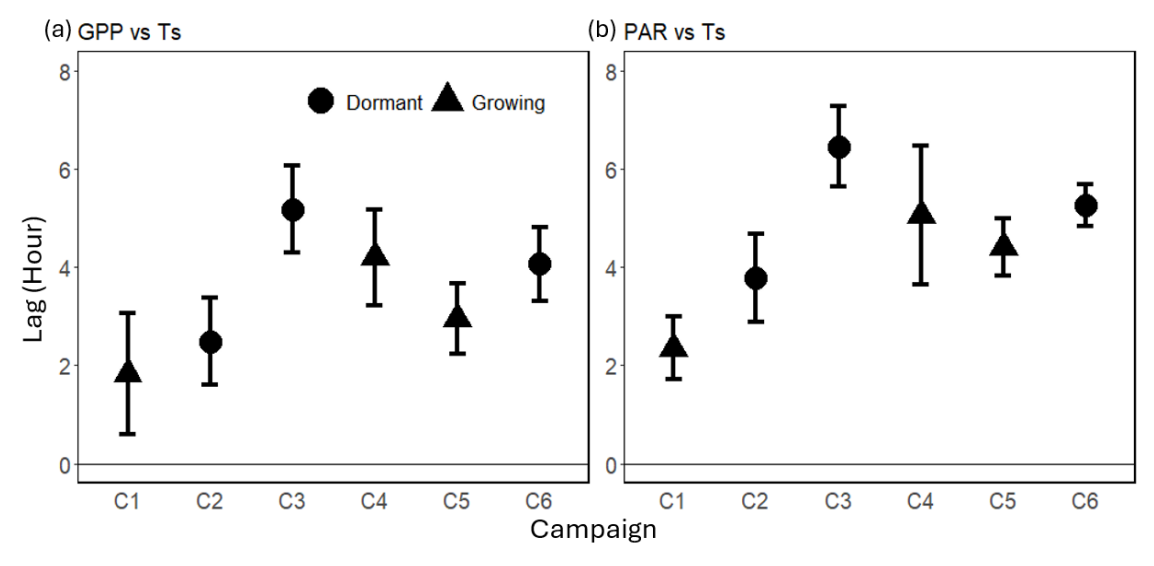


Figure S13. Mean lag times (\pm standard deviation) between (a) gross primary productivity (GPP) and soil temperature (Ts_5), and (b) photosynthetically active radiation (PAR), and Ts_5 at the diurnal frequency range (0.5 to 1.5 d) across six measurement campaigns (C1–C6). Phase differences were averaged over the diurnal frequency range and included only when the 1 d spectral peak was significant (p < 0.1). Circular dots represent dormant season campaigns, while triangles represent growing season campaigns. Positive lag values indicate that GPP or PAR lagged behind Ts_5 , while negative values indicate that GPP or PAR preceded Ts_5 .